Ammonium Glycyrrhizinate Protects Gastric Epithelial Cells from Hydrogen Peroxide-Induced Cell Death

Hyun-Mee Oh, SungGa Lee, Young-Na Park, Eun-Ju Choi, Ji-Young Choi, Jeong Ah Kim, Ji-Hye Kweon, Weon-Cheol Han, Suck-Chei Choi, Joung-Kyue Han, Jong-Keun Son, Seung-Ho Lee and Chang-Duk Jun

Exp Biol Med (Maywood) 2009 234: 263
DOI: 10.3181/0805-RM-178

Ammonium Glycyrrhizinate Protects Gastric Epithelial Cells from Hydrogen Peroxide-Induced Cell Death

Hyun-Mee Oh,*,† SungGa Lee,* Young-Na Park,* Eun-Ju Choi,* Ji-Young Choi,‡ Jeong Ah Kim,‡ Ji-Hye Kweon,§ Weon-Cheol Han,§ Suck-Chei Choi,§ Joung-Kyue Han,|| Jong-Keun Son,‡ Seung-Ho Lee,‡ and Chang-Duk Jun*,†,¶,[1]

Department of Life Sciences, and †Cell Dynamics Research Center, GIST, Gwangju 500–712, Korea; ‡College of Pharmacy, Yeungnam University, Gyeongsan 712–749, Korea; §Digestive Disease Research Institute, Wonkwang University School of Medicine, Iksan, Chonbuk 570–749, Korea; ||Department of Physical Education, Chung-Ang University, Seoul 156–756, Korea; and ¶Research Center for Biomolecular Nanotechnology, GIST, Gwangju 500–712, Korea

Glycyrrhiza uralensis **has a potential for preventing or ameliorating gastric mucosal ulceration. To understand the molecular mechanism about the medicinal effect of *G. uralensis*, we isolated four single compounds from *G. uralensis* and one related compound and screened for the cellular protective effect against H_2O_2-induced damage in gastric epithelial AGS cells. Interestingly, we found that ammonium glycyrrhizinate (AG) prepared from glycyrrhizin dramatically protects AGS cells from H_2O_2-induced damage as measured by the integrity of actin cytoskeleton. AG also inhibited $FeSO_4$-induced reactive oxygen radicals in a dose-dependent manner, suggesting the role for AG as a free radical scavenger. To better understand the protective role of AG at the transcriptional level, we performed genome-wide expression profiling using high-density oligonucleotide microarrays, followed by validation using RT-PCR. Among the 33,096 genes that were screened in the microarray, 936 genes were found to be differentially expressed in a statistically significant manner in the presence or absence of H_2O_2 and AG. Among the 936 genes, 51 genes were differentially expressed at least 3-fold in response to the H_2O_2 treatment. AG blocked the expression of genes related to apoptotic cell death (GDF15, ATF3, TNFRSF10A, NALP1) or oxidative stress pathways (HMOX1) which was elevated in response to H_2O_2 treatment, suggesting a potential protective role for AG in oxidative stress-induced cell death. Collectively, current results demonstrate that AG is a novel antioxidant that could be effective for the treatment of gastric diseases related to the oxidative stress-induced mucosal damage.** Exp Biol Med 234:263–277, 2009

Key words: *Glycyrrhiza uralensis*; ammonium glycyrrhizinate; AGS; reactive oxygen radicals

Introduction

Reactive oxygen species (ROS) are a class of highly reactive molecules derived from the metabolism of oxygen. ROS can play a central role in regulating cell proliferation and cell death. ROS, such as superoxide and hydrogen peroxide, have been shown to influence cell death triggered by internal cues (p53-mediated), external cues (TGF-β-mediated) and immunogenic signals (TNF-α) (1–3). ROS can also cause extensive damage to cells and tissues and disrupt the barrier function of epithelium (4–6). For instance, ROS increases the permeability of cultured epithelium (5). The increase in permeability is associated with morphological changes in the cells, such as separation of adjacent cells and disruption of the actin cytoskeleton (5).

The gastric epithelium is continuously exposed to toxic ROS generated within the gastric lumen (ingested food, cigarette smoke, etc.). In addition, the gastritis associated with *H. pylori* infection stimulates the generation of ROS by inflammatory cells present in the mucosa (7–9). Protection of cells against ROS is accomplished through the activation of oxygen-scavenging enzymes such as superoxide dismutase, catalase, and glutathione peroxidase (10). However, impairment of this important host-cell defense mechanism would greatly reduce the ability of the gastric epithelial cells to tolerate environmental ROS, such as those present with the chronic gastritis associated with *H. pylori* infection (7,

This work was supported by grants from the Basic Research Program (R01-2008-000-20989-0) and the SRC program (R11-2007-007-01002-0) of MOST/KOSEF, and the Research Program (2008-C00265) of Korea Research Foundation.

[1] To whom correspondence should be addressed at Department of Life Sciences, GIST, Gwangju 500–712, Korea. E-mail: cdjun@gist.ac.kr

Received May 28, 2008.
Accepted December 26, 2008.

DOI: 10.3181/0805-RM-178
1535-3702/09/2343-0263$15.00

8). Thus, disturbance of the oxidant-antioxidant balance in the stomach might greatly increase the risk of cell death or DNA damage from ROS.

With a 3000-year history of use as a medicinal plant, *Glycyrrhiza uralensis* (Leguminosae) is one of the oldest herbal medicines known and has been studied extensively. Interestingly, water-extracted *G. uralensis* is known to reduce gastric ulcers *in vitro* and *in vivo* (11–13). Glycyrrhizin, an active agent in *G. uralensis*, has been thoroughly studied and known to exhibit a number of pharmacological effects against inflammation, ulcers, allergies, and carcinogenesis (12–14). Glycyrrhizin is commonly used in Japan and is now under therapeutic trial in Europe in patients with chronic hepatitis (15, 16), and its ammonium salt (ammonium glycyrrhizinate) is used as an anti-inflammatory and anti-allergic remedy (13). Moreover, new anti-inflammatory and anti-ulcer agents are found among glycyrrhizin derivatives such as esters, amides, ureids, carbamates, thioureids and glycopeptides (13). Glycyrrhizin glycopeptides are also of interest as immunomodulators (13). Some of the chemically modified glycyrrhizin derivatives (salts, amides, glycopeptides) are potent HIV-1 and HIV-2 inhibitors *in vitro* (13). However, the mechanisms by which these compounds exert their therapeutic effects are largely unknown and less research has been conducted on whether these compounds have antioxidative effects in gastric epithelial cells.

In this study, we screened five compounds. Four of these compounds, liquiritigenin (LG), ononin (ON), glycyrol (GC), and glycyrrhizin (GR), were isolated from *G. uralensis* and one, ammonium glycyrrhizinate (AG), was prepared from glycyrrhizin. We measured their activity in preventing H_2O_2-induced actin disruption in gastric epithelial AGS cells. We found that AG potently blocked H_2O_2-induced actin disruption, thereby protecting cells from damage. To explore more precisely the effect of AG on H_2O_2-induced cell damage, we employed a DNA microarray to examine the patterns of global gene expression in AGS cells. We found a number of differentially expressed genes between untreated controls and H_2O_2-treated AGS cells. We also found that AG blocked the expression of several genes related to apoptotic cell death and oxidative stress pathways which was markedly up-regulated by H_2O_2 treatment.

Materials and Methods

Reagents. Hydrogen peroxide, dimethyl sulfoxide (DMSO), phosphate-buffered saline (PBS), TRITC-Phalloidin, and 3-(4,5-dimethylthiazol-2-yl)-2,5-diphenyltetrazolium bromide (MTT) were purchased from Sigma Chemical Co. (St. Louis, MO). Dihydrorhodamine 123 (DHR) was from Molecular Probes, Inc. (Eugene, OR). Propidium iodide (PI) and DAPI were purchased from Calbiochem-Behring Corp. (La Jolla, CA). Five compounds from *Glycyrrhiza uralensis* were prepared as described before (15–21) and dissolved in DMSO at a concentration of 100 mg/ml, stored at –20°C, protected from light, and thawed immediately before use.

Cell Culture. Human gastric epithelial AGS cells obtained from the American Type Culture Collection (ATCC) were cultured at 37°C in a 5% CO_2 atmosphere in Ham's F12 medium supplemented with heat-inactivated 10% fetal bovine serum (FBS; Gibco BRL) and appropriate antibiotics.

Plant Material. The roots of *G. uralensis* (Leguminosae) were purchased in Taegu, Korea. The identity of a specimen of the root was verified by Je-Hyun Lee, PhD, at Kyung Hee University in Korea.

Isolation of Compounds from *G. uralensis*. The roots of *G. uralensis* (10 kg) were extracted with methanol (50 L) at room temperature. The methanol extract was evaporated under reduced pressure to obtain a residue (2.6 kg), which was dissolved in water (3.5 L) and partitioned with methylene chloride (3.5 L X 3). The methylene chloride soluble fraction (fr.; 230 g) was separated by chromatography on silica gel (6.2 kg), eluting with n-hexane, gradually increasing the polarity with ethyl acetate (100:0, 98:2, 95:5, 90:10, 85:15, 80:20, 5 L for each gradient) to give 16 fractions. As previously described, fr. 4 (3200 ml, n-hexane-ethyl acetate, 98:2) and fr. 8 (1200 ml, n-hexane-ethyl acetate, 90:10) were crystallized from cold methanol to yield glycyrol (450 mg, 90% pure) (17). Fr. 9 (2400 ml, n-hexane-ethyl acetate, 90:10) was re-separated by chromatography over silica gel (300 g), eluting with methylene chloride-MeOH (1.5 L) to give liquiritigenin (300 mg, 100% pure) (18). Fr. 12 (3600 ml, n-hexane-ethyl acetate, 80:20) was separated over silica gel (700 g), eluting with methylene chloride-MeOH (95:5, 2 L) to give ononin (70 mg, 92% pure) (19) and glycyrrhizin (950 mg, 98% pure) (20). The chemical structures were identified by comparing spectral data and hydrolysates of these compounds with those of authentic samples. The chemical structures of four compounds are shown in Figure 1A.

Preparation of Ammonium Glycyrrhizinate (AG). AG was prepared according to Kondratenkos's method (21–23). An acetone solution (10 ml) of glycyrrhizin (800 mg) was gradually stirred into a 25% NH_4OH solution to a pH of ~8–8.5. The reaction mixture was filtered and washed with ethanol and dried in air to obtain 600 mg of reaction product. This product was heated with 3 ml of glacial AcOH, washed with ethanol, and recrystallized by 85% ethanol to obtain 520 mg of pure ammonium glycyrrhizinate (99% pure); ^{1}H-NMR (250 MHz, DMSO-d_6) δ: 5.37 (1H, s, H-12), 4.47 (1H, d, J = 7.8 Hz, H-1′), 4.29 (1H, d, J = 7.8 Hz, H-1"), 1.25, 1.23, 1.22, 1.17, 1.13, 1.08, 0.83 (each 3H, s, 7CH_3), ^{13}C NMR (62.5 MHz, DMSO-d_6) δ: 199.5 (C-11), 179.1 (C-30), 172.7 (C-13), 172.5 (C-6"), 169.6 (C-6′), 128.4 (C-12), 106.2 (C-1"), 105.2 (C-1′), 90.9 (C-3), 84.0 (C-2′), 78.0 (C-2"), 77.7 (C-3′), 77.2 (C-3"), 76.7 (C-4′), 76.2 (C-4"), 73.3 (C-5"), 73.0 (C-5′), 61.7 (C-9), 55.0 (C-5), 48.6 (C-18), 46.8 (C-14),

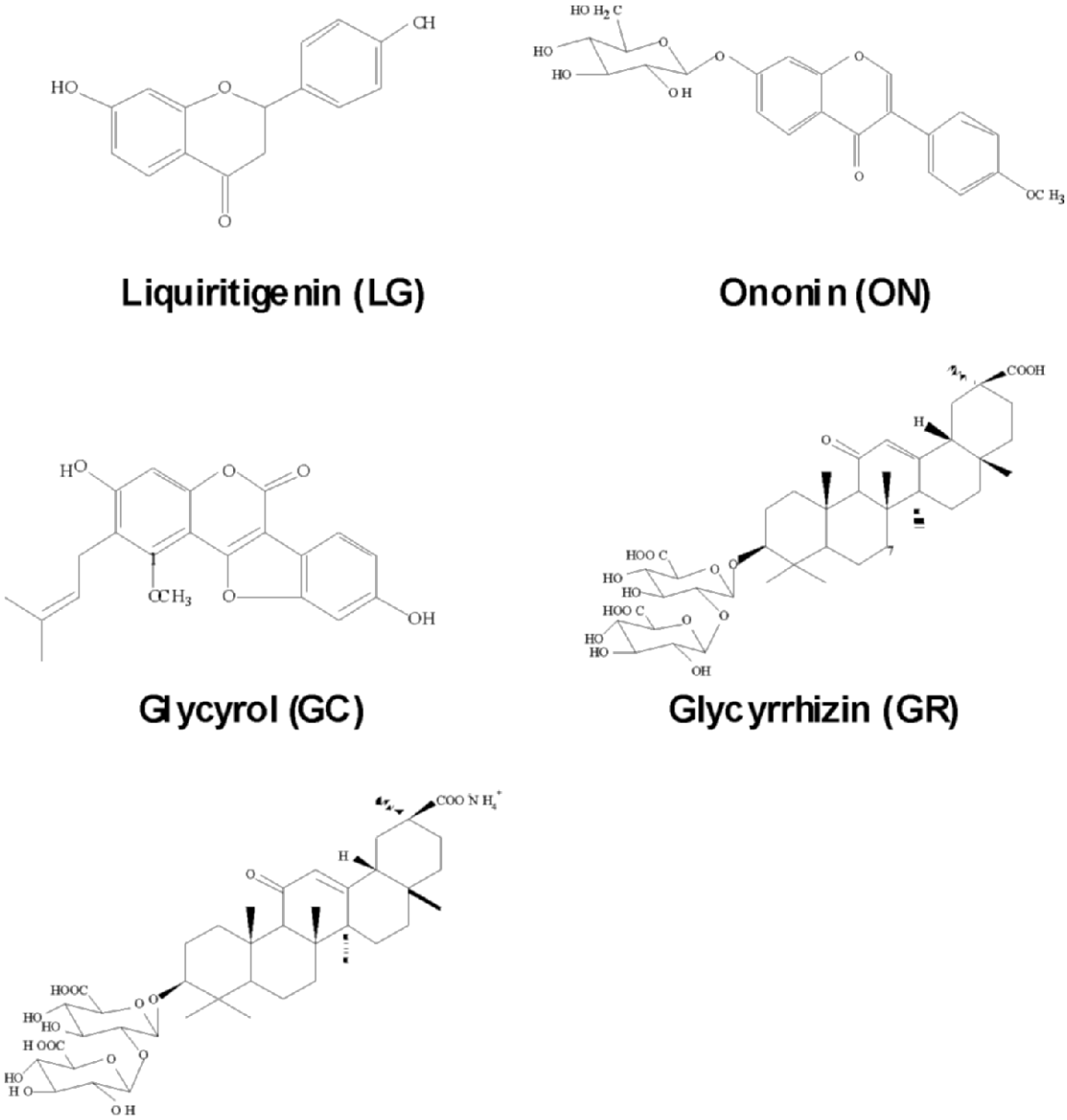

Figure 1. Chemical structure of compounds isolated from *G. uralensis* and of ammonium glycyrrhizinate (AG).

45.4 (C-20), 44.0 (C-8), 43.4 (C-19), 40.5 (C-4), 40.3 (C-1), 38.3 (C-22), 37.1 (C-10), 33.8 (C-7), 33.0 (C-17), 32.0 (C-21), 29.2 (C-29), 28.8 (C-28), 28.3 (C-23), 27.6 (C-2), 27.4 (C-16), 27.0 (C-15), 23.5 (C-27), 18.6 (C-26), 17.1 (C-6), 16.8 (C-25), 16.6 (C-24). The chemical structure and HPLC chromatogram of purified AG is shown in Figure 1A and B.

Actin Staining of AGS Cells. The AGS cells (2×10^5/well) were grown on glass coverslips (18-mm diameter; Fisher Scientific, Pittsburgh, PA). The culture medium was freshly replaced 1 h before reagent treatment. The cells were pretreated for 30 min with the compounds (AG, CD, ON, LG, and GC) isolated from *Glycyrrhiza uralensis,* and then treated with H_2O_2 for 1 h at 37°C. The cells were fixed for 15 min with 3.7% paraformaldehyde in PBS containing 0.1% Triton X-100 and 1 mM $MgCl_2$ (pH 7.2), stained with TRITC–phalloidin in PBS, and mounted with anti-fade solution (Molecular Probes). The slides were examined with an FV1000 confocal laser scanning microscope (Olympus Corporation, Japan) equipped with ×40, ×60, and ×100 objectives and the data were analyzed by using FLUOVIEW software, version 1.5 (Olympus Corporation, Japan).

Measurement of ROS. The production of ROS was measured by detecting the fluorescent intensity of oxidant-sensitive probe dihydrorhodamine 123 (DHR, Molecular Probes) (24). Cells (2×10^5/well in 96-well plates) were washed with Lock's buffer and incubated with AM-DHR at

37°C/5% CO_2 for 30 min. The cells were then incubated with AG in the presence or absence of $FeSO_4$. After 30 min of incubation, the kinetics of fluorescent intensity for DHR was recorded using fluorescent plate reader at excitation of 507 nm and emission of 529 nm. The fluorescent readings were digitized using SoftMax Pro (Molecular Devices, Sunnyvale, CA). The results were similar in three independent experiments and data from a representative experiment ($n = 5$ replications) have been illustrated.

Cell Viability Assay. Cellular viability was evaluated by the reduction of MTT to formazan. A stock solution of MTT was prepared in PBS, diluted in Ham's F12 medium, and added to cell-containing wells at a concentration of 0.5 mg/mL after the culture medium was first removed. The plates were then incubated for 4 h at 37°C in 5% CO_2. At the end of the incubation period, the medium was aspirated, and the formazan product was solubilized with dimethyl sulfoxide. Absorbency was measured on a multiscan reader with a 570 nm wavelength filter.

RNA Isolation. AGS cells (2×10^6) were grown in 60-mm culture dish for 12 h and then were incubated for 1 h with vehicle (0.05% DMSO), AG (50 μg/ml), H_2O_2 (0.3 mM), or AG plus H_2O_2. In case of simultaneous treatment, cells were treated with AG before H_2O_2 unless otherwise indicated. Then, the cells were washed and incubated for 6 h with fresh complete medium containing 10% FBS. Cells were harvested and total RNA was isolated from cells using easy Blue (iNtRON Biotechnology, Korea), following the manufacturer's instructions. The total RNA samples were measured for quality at 260/280 nm, 260/230 nm, and 28S/18S ratio.

cDNA Preparation and Microarray Hybridization. For each hybridization, dUTP-labeled cDNA was amplified from total RNA samples (5 μg per sample) by RT-IVT Labeling Reagents (Applied Biosystems, MA). Fifty μg of labeled cDNA were subsequently purified by using RT-IVT Purification Components (Applied Biosystems). The resulting samples were hybridized on a microarray chip containing oligonucleotide probes for 33,096 human genes (Applied Biosystems) and further processed according to the Applied Biosystems protocol.

DNA Microarray Analysis. Microarray images were acquired with an AB 1700 microarray analyzer (Applied Biosystems). Signal quantification and data processing were performed using AVADIS (Strand Genomics, India). Each experiment was repeated three times to reduce the risk of false-positive or false-negative results. The results from three independent identical experiments were merged, and the merged data were used for subsequent comparisons. The average intensity values for each gene were calculated. Significant differences in gene expression between the data obtained from the four different groups (control, AG, H_2O_2, and AG plus H_2O_2) were identified using the one-way ANOVA Kruskal-Wallis Test with a significance threshold of $P < 0.05$. The K-means clustering method was used to cluster those genes selected by the above test. To estimate fold induction, the ratios of treated- to untreated-signal intensities were calculated. The $\log_2$ of each ratio was determined to equalize the magnitude of deflection of up-regulated and down-regulated genes, and the differences in gene expression were ranked based on absolute values.

Semiquantitative RT-PCR. Semiquantitative RT-PCR was performed to validate the gene expression data from microarray analysis. Each set of samples was analyzed in triplicate. The RNA samples used in RT-PCR experiments were identical to those used in microarray experiments. Reverse transcription of the RNA was performed using the RT PreMix Kit (iNtRON Biotechnology). One microgram of RNA and 20 pmol primers were preincubated at 70°C for 5 min and transferred to a mixture tube. The reaction volume was 20 μl. cDNA synthesis was performed at 42°C for 60 min, followed by RT inactivation at 94°C for 5 min. Thereafter, the RT-generated DNA (2–5 μl) was amplified using the PCR PreMix Kit (iNtRON Biotechnology). The primers used for cDNA amplification were: 5′-ATGACTTCCAAGCTGGCCGTGGCT-3′ (sense) and 5′-TCTCAGCCCTCTTCAAAAACTTCTC-3′ (antisense) for GDF15; 5′-ATGTGCTGTACCAAGAGTTTG-3′ (sense) and 5′-TTACATGTTCTTGACTTTTTTACTGAGGAG-3′ (antisense) for ATF3; 5-ACTATACTTCCCGAGGCATCCTT-3 (sense) and 5-TGGTCTTGGAAGTCAGTGTGAGT-3 (antisense) for NALP1; 5′-CAGAACATCCTGGAGCCTGTAAC-3′ (sense) and 5′-ATGTCCATTGCCTGATTCTTTGTG-3′ (antisense) for TNFRSF10A; 5′-CGGAGTCAACGGATTTGGTCGTAT-3′ (sense), 5′-AGCTTCTCCATGGTGGTGAAGAC-3′ (antisense) for HMOX1; and 5′-CGGAGTCAACGGATTTGGTCGTAT-3′ (sense), 5′-AGCTTCTCCATGGTGGTGAAGAC-3′ (antisense) for GAPDH. Amplification conditions were denaturation at 94°C for 30 s, annealing at 56°C for 30 s, and extension at 72°C for 30 s for 30 cycles. The expected PCR products were 120 bp (for GDF15), 540 bp (for ATF3), and 301 bp (for NALP1), 299 bp (for TNFRSF10A), 265 bp (for HMOX1), and 306 bp (for GAPDH). PCR products were subjected to electrophoresis on 1.2% agarose gel and were stained with ethidium bromide.

Real-Time Quantitative PCR. Real-time RT-PCR was performed to quantify the expression levels of TNFRSF10A, HMOX1 and NALP1, GDF15, ATF3 mRNA. The mRNA levels were analyzed by quantitative real-time RT-PCR using DNA Engine with Chromo-4 Detector (MJ Research, Waltham, MA). Total RNAs isolated using easy Blue (iNtRON Biotechnology, Korea) was reverse transcribed to cDNA using RT PreMix Kit (iNtRON Biotechnology). Obtained cDNA was subjected to quantitative real-time PCR in accordance with the manufacturer's instructions with modifications. PCR was performed in triplicate using 12.5 μl of SYBR Premix Ex Taq (Takara, Japan) and 2 μl of cDNA as a template in a 25 μl of final volume. PCR amplification was preceded by incubation of the mixture for 15 min at 95°C and the 40 cycles of

the amplification step consisted of denaturation, annealing and extension. The denaturation was performed for 30 s at 95°C, annealing was done in a transitional temperature range from 58°C to 62°C with a step-size of 0.5°C per cycle and the extension was performed 30 s at 72°C with fluorescence detection at 72°C after each cycle. After the final cycle, melting-point analyses of all samples were performed within the range from 65°C to 95°C with continuous fluorescence detection. Expression level of GAPDH was used for normalization.

Apoptosis Assay. Two methods were used to identify apoptotic cells. The first method involved fluorescent imaging of cells labeled with DAPI dye. Cells treated with various agents were cytospun, fixed in 4% neutral buffered paraformaldehyde, and permeabilized with PBS/0.5% Triton X-100, and their nuclei were stained for 5 min with DAPI dye. The coverslips were then washed, mounted onto slides, and viewed with a fluorescence microscope. The second method involved the flow cytometric analysis (25). Approximately 10^5 cells per experimental condition were harvested, washed with HBSS, and sequentially resuspended in a solution containing 0.1% Nonidet P-40 and 50 μg/ml PI. The content of DNA per cell was estimated by flow cytometry on a FACSCalibur (Becton Dickinson, San Jose, CA) and analyzed on associated CellQuest (Becton Dickinson) software. All experiments were performed at least three times unless otherwise indicated.

Statistics. The mean values were calculated from data taken from at least three (usually three or more) separate experiments conducted on separate days. Where significance testing was performed, an independent *t* test (Student's *t* test; two populations) was used. A *P* value less than 0.05 was considered to indicate statistical significance.

Results

Effects of Five Compounds from *G. uralensis* on H_2O_2-Induced Actin Disruption of Gastric Epithelial AGS Cells. H_2O_2 has been known to induce loss of actin cytoskeletal integrity in various cell types including mucosal epithelial cells (4, 5, 26). In this study, we selected gastric epithelial AGS cells to investigate the effects of single compounds (isolated from *G. uralensis* or prepared from glycyrrhizin (Fig. 1)) because these cells are highly susceptible to H_2O_2 and that a low dose of H_2O_2 (0.3 mM) significantly induces morphological changes along with the increased actin disruption (Fig. 2A). Interestingly, pretreatment of AGS cells with AG (10–100 μg/ml) dramatically blocked H_2O_2-induced cytoskeleton changes, as determined by TRITC-phalloidin staining (Fig. 2B, top). In contrast, treatment of cells with other single compounds such as LG, ON, GC, and GR showed a little protecting effect against H_2O_2-induced actin disruption (Fig. 2B, bottom). Based on these results, we hypothesized that the effect of AG to protect H_2O_2-induced actin cytoskeletal changes are associated with its efficacy to scavenge ROS generated within the cells or derived from a variety of external sources. We therefore further examined whether AG inhibits ROS generation in AGS cells stimulated by $FeSO_4$ (150 μM) (24). As shown in Figure 3A, treatment with AG dramatically inhibited $FeSO_4$-induced ROS production in a dose-dependent manner and the inhibition levels were comparable to that of achieved with N-acetyl-L-cysteine (NAC), a free radical scavenger. The concentrations ranging from 10 to 500 μg/ml of AG showed no toxic effects at 24 h of incubation on AGS cells (Fig. 3B).

Modulation of Gene Expression in Response to H_2O_2 With or Without AG. In order to understand the protective role of AG at the transcriptional level in H_2O_2-treated AGS cells, we analyzed the global gene expression patterns of AGS cells that were treated for 1 h with H_2O_2 (0.3 mM) alone, AG (50 μg/ml) alone, and AG plus H_2O_2. The expression profiles were surveyed through microarray experiments and a data analysis procedure of microarray is as follows: extracting quantification data from images, filtering data with standards (flag value < 5000, signal-to-noise (SN) ratio > 3), normalizing $\log_2$ ratios, identifying differentially expressed genes (one-way ANOVA test with $P < 0.05$), clustering genes (K-mean clustering), sorting of interesting genes (3-fold change of expression, functional classification), and expression validation by RT-PCR (Fig. 4).

To show an overview of the expression profiles of our samples, we generated scatter plots (13,669 genes) of comparative data after filtration and normalization of signals (Fig. 5). The lack of concordance between the control group and the H_2O_2-treated group indicates that the expression of numerous genes is altered in AGS cells by H_2O_2 treatment. In contrast, comparison of the control group with the AG-treated group revealed a high degree of concordance (Fig. 5), suggesting that AG has a modest effect on gene regulation in resting AGS cells. AG plus H_2O_2-treated samples showed higher concordance of gene expression with the control group than with the H_2O_2-treated group (Fig. 5).

We then performed one-way ANOVA Kruskal-Wallis test to identify the genes that are differentially expressed in a statistically significant manner between the data obtained from the four different groups (control, AG, H_2O_2, and AG plus H_2O_2). The statistical test revealed that 936 genes were differently expressed ($P < 0.05$) and then the results were displayed by dendrogram (Fig. 6). The green blocks represent the down-regulated genes, the red blocks represent up-regulated genes, and the black blocks represent the genes that are not altered relative to the control. These genes could be clustered into nine patterns of expression that were statistically related by the K-means clustering method. The three clusters (clusters 2, 3, and 8) were changed most significantly in response to H_2O_2 treatment. Cluster 2 (157 genes) showed the genes that are down-regulated by AG treatment but significantly up-regulated by H_2O_2 treatment (fold changes, FC: >1 and ≤ 7). Cluster 3 (155 genes)

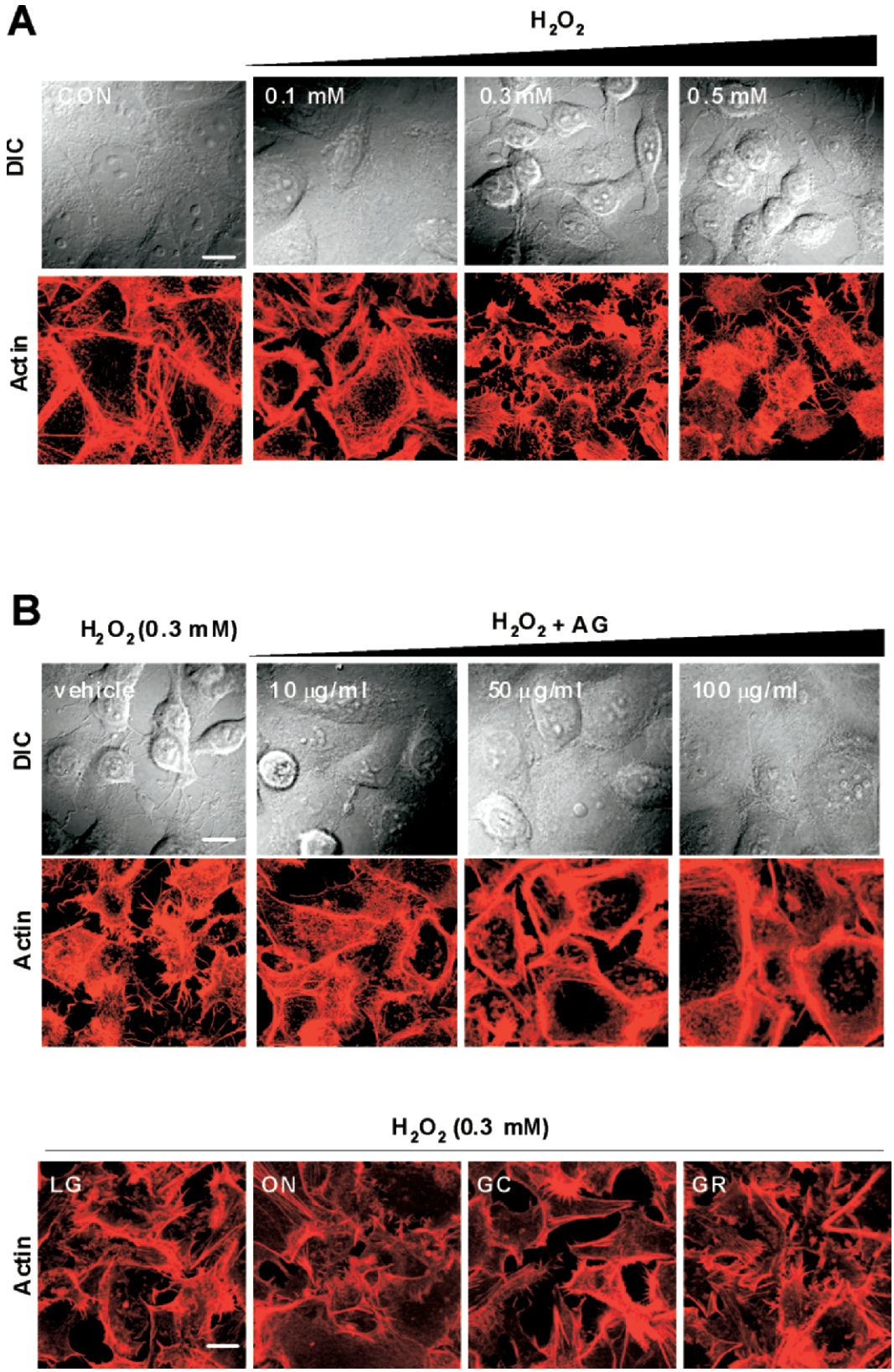

Figure 2. Effect of five compounds from *G. uralensis* on H_2O_2-induced actin disruption in cultured AGS cells. (A) AGS cells (2×10^5/well) were grown on glass coverslips. The cells were incubated with various concentrations (0.1–0.3 mM) of H_2O_2 for 1 h at 37°C. After incubation, cells were fixed and stained with TRITC-phalloidin as described in Materials and Methods. The slides were examined with a FV1000 confocal laser scanning microscope (×40), and the data were analyzed by using the FLUOVIEW software ver. 1.5. Bar, 10 μm. (B) AGS cells were pretreated for 30 min with 10–100 μg/ml of AG or 50 μg/ml of LG, ON, GC, and GR, and then incubated with 0.3 mM of H_2O_2 for 1 h at 37°C. F-actin was examined as described in A. The results were similar in three independent experiments. A color version of the figure is available in the online journal.

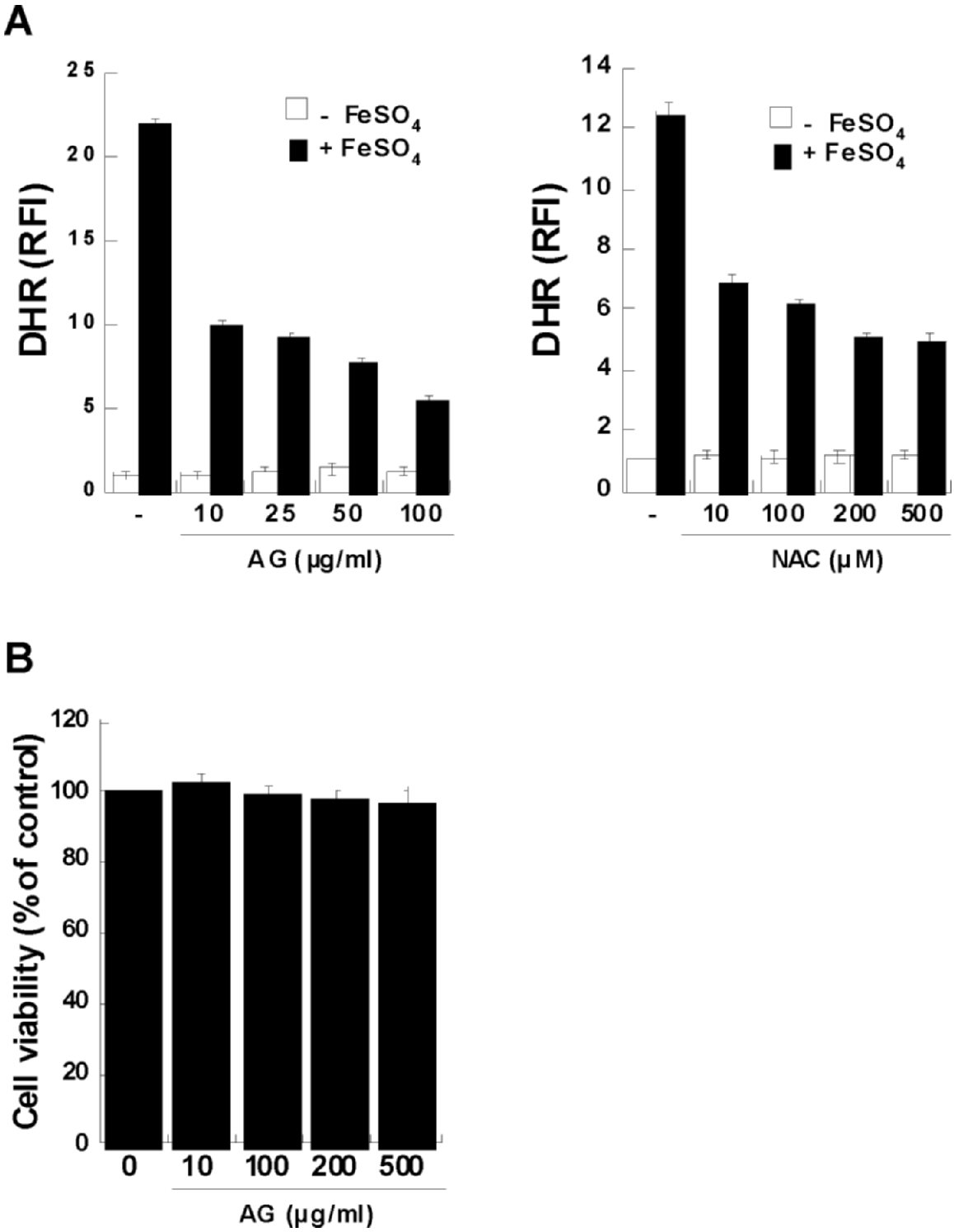

Figure 3. Effect of AG on $FeSO_4$-mediated ROS generation in cultured AGS cells. (A) Cells (2×10^5/well) were incubated with the various concentrations of AG (10–100 μg/ml) or N-acetyl-L-cysteine (NAC; 10–500 μg/ml) in the presence or absence of $FeSO_4$ (150 μM). After 30 min, the fluorescent intensity for DHR was recorded using fluorescent plate reader at excitation of 507 nm and emission of 529 nm. The data shown represent the mean ± SD of three independent experiments. (B) AGS cells were treated with various concentrations of AG (0–100 μg/ml) for 24 h. Quantitative analysis of cell viability was determined by the MTT assay (mean ± SD, $n = 3$).

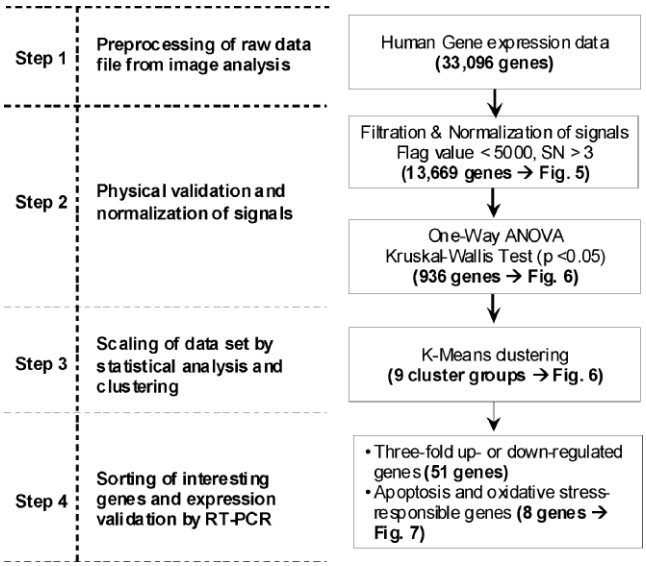

Figure 4. Schematic of the process used to analyze microarray data.

showed the genes that are not changed by AG treatment but highly up-regulated by H_2O_2 treatment (FC: >1 and ≤ 7). Additionally, cluster 8 (6 genes) revealed the genes that are not significantly changed by AG treatment but most highly up-regulated by H_2O_2 treatment (FC: >7).

The genes selected by the above test were further filtered to identify candidates for which the expression levels differed by at least 3-fold between the control and H_2O_2-treated groups. Among the 936 genes, 51 genes were differentially expressed at least 3-fold in response to treatment with H_2O_2. Among these 51 genes, 43 genes were up-regulated and 8 genes were down-regulated relative to control. The known individual genes, which were up-regulated by H_2O_2 treatment, except for 6 unknown genes, were listed in Table 1. However, down-regulated genes were mostly unassigned hypothetical genes (data not shown). The up-regulated genes were then separated by biologic process categories and those genes involved in apoptotic cell death and/or oxidative stress pathways were selected for additional study (Fig. 7). Seven up-regulated genes, including GDF15, ATF3, TNFRSF10D, CDKN1A, NALP1, TNFRSF10A, and FOXO3A, had an assigned biological process of apoptotic cell death (Fig. 7A). These genes are known to be involved in the prevention or induction of apoptosis in several cell types. For instance, GDF15, ATF3, NALP1, and TNFRSF are known inducers of apoptosis in various biological systems (27–29). Those pro-apoptotic genes up-regulated by H_2O_2 treatment were all blocked by AG treatment (Fig. 7A and B). Additionally, AG also significantly blocked the expression of heme

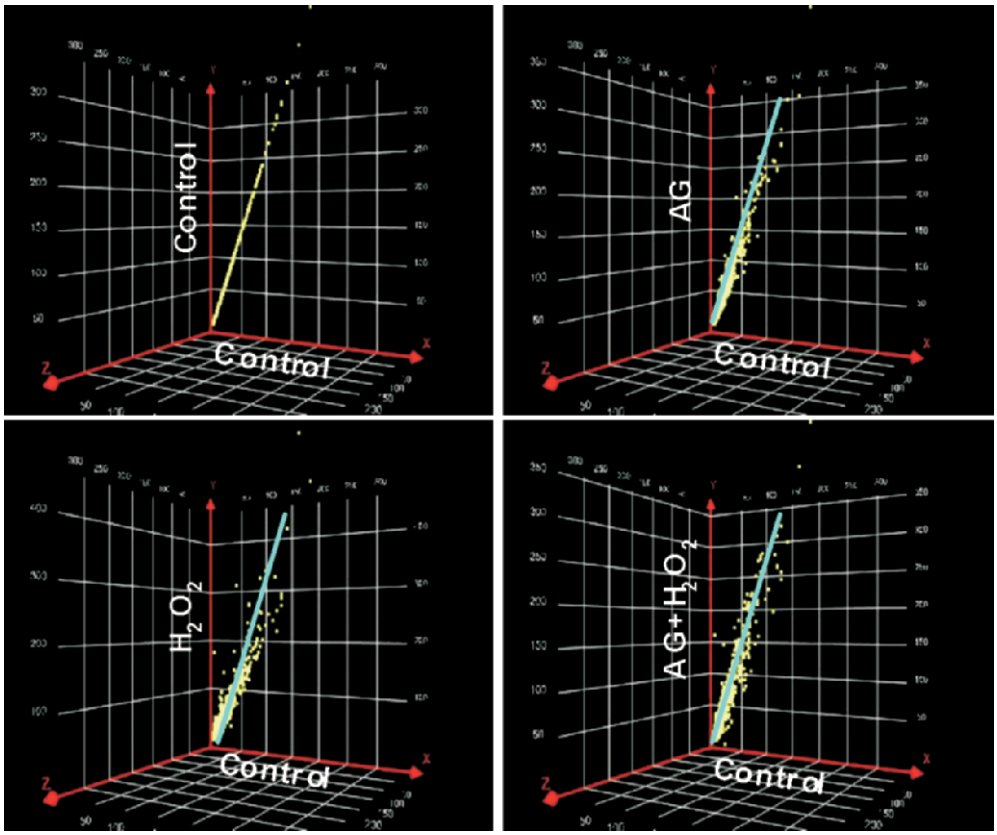

Figure 5. Scattering diagrams of control: control, control: H_2O_2, control: AG, and control: AG plus H_2O_2. AGS cells were treated as described in Materials and Methods. Total RNA was isolated and analyzed by DNA microarray hybridization. The central diagonals on each scatter plot represent no change from the control state (untreated). The upper and lower diagonals represent expression changes from the control state. A color version of the figure is available in the online journal.

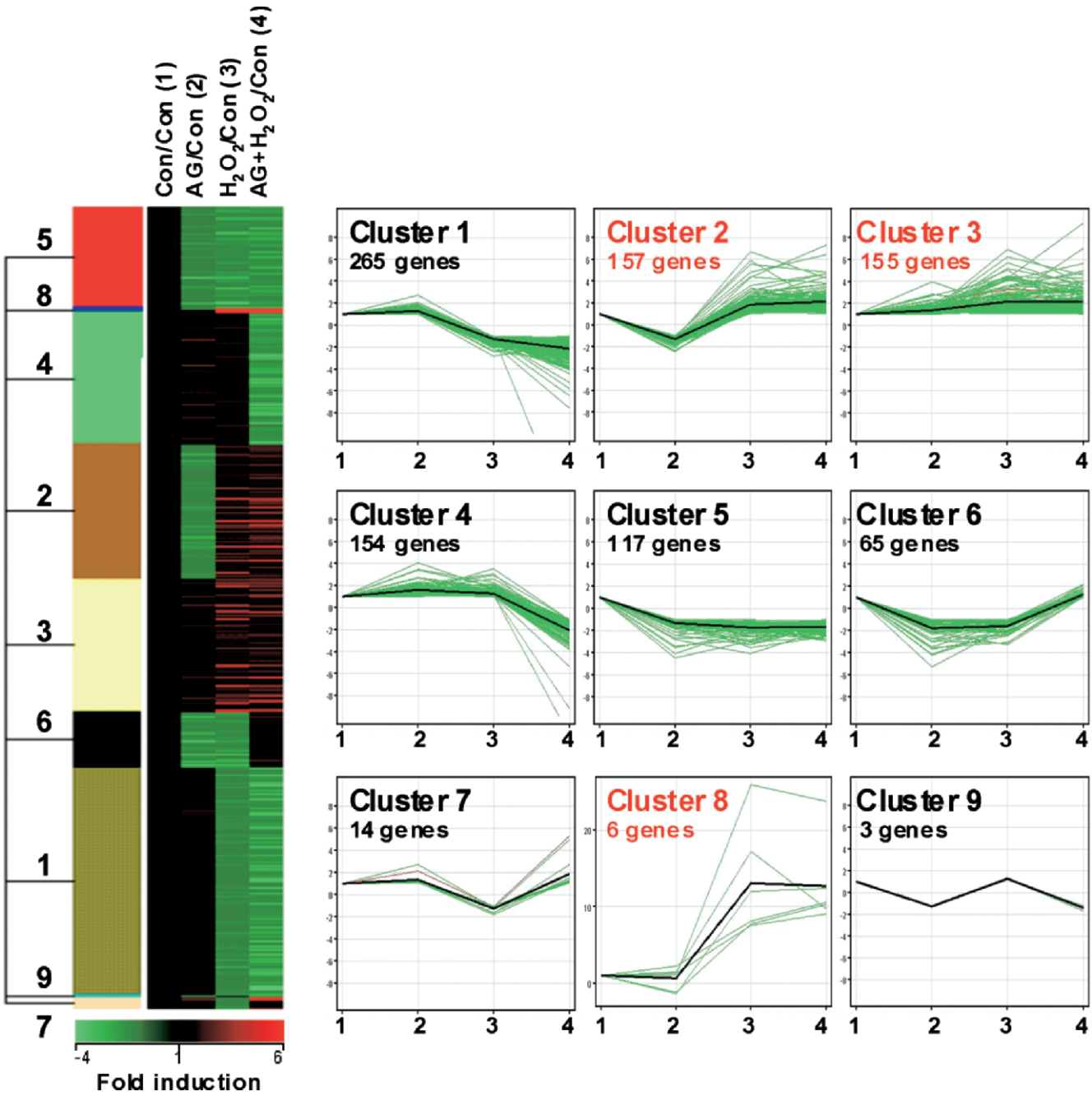

Figure 6. Dendrogram and K-means clustering analysis of gene expression profiles in AGS cells treated with AG, H_2O_2, or AG plus H_2O_2 (total 936 genes). The gene expression matrix for the cluster algorithm contains the log-transformed medians of normalized ratios. Up-regulated genes are depicted in shades of red, down-regulated genes in shades of green. Genes with similar expression patterns are clustered together. Clusters selected for further analysis are indicated in red in the right panel. A color version of the figure is available in the online journal.

oxygenase-1 (HMOX1) related to oxidative stress pathways which was up-regulated more than 4-fold by H_2O_2 treatment (Fig. 7A and B). Since it is well identified that HMOX1 is an oxidative stress-responsible gene and the expression is induced by exposing to ROS generated within the cells or derived from a variety of external sources (30, 31), the inhibition of HMOX1 expression by AG further evidences that AG scavenges ROS generated from H_2O_2. We further validated the specific up- or down-regulation of these selected genes with RNA samples used for the microarray experiments. The results of both RT-PCR and real-time PCR suggested that the expression pattern of these genes agrees with those observed in the microarray experiments.

AG Protects AGS Cells from H_2O_2-Induced Apoptotic Cell Death. We finally tested whether AG has a protective effect on H_2O_2-induced apoptotic cell death. Within 12 h after exposure to the H_2O_2 (0.3 mM), 45% of AGS cells underwent apoptotic cell death, as

Table 1. Genes Whose Expression Was Increased More than 3-Fold in Response to H_2O_2[a]

Gene name	Gene symbol	RefSeq_NM	Fold change[b]			
			AG/con	H_2O_2/con	AG + H_2O_2/con	H_2O_2/AG + H_2O_2
Growth differentiation factor 15	**GDF15**	**NM_004864**	**1.14**	**24.38**	**11.64**	**2.09**
Activating transcription factor 3	**ATF3**	**NM_004024**	**1.10**	**17.10**	**7.75**	**2.21**
Phorbol-12-myristate-13-acetate-induced protein 1	PMAIP1	NM_021127	2.27	8.11	10.55	−1.30
Serine (or cysteine) proteinase inhibitor, clade B (ovalbumin), member 2	SERPINB2	NM_002575	−1.16	7.71	10.35	−1.34
Early growth response 1	EGR1	NM_001964	1.31	7.60	9.11	−1.20
Plasminogen activator, urokinase receptor	PLAUR	NM_001005377	1.35	6.90	3.36	2.05
Tumor necrosis factor receptor superfamily, member 10d	**TNFRSF10D**	**NM_003840**	**−1.32**	**6.69**	**4.28**	**1.56**
Cyclin-dependent kinase inhibitor 1A	**CDKN1A**	**NM_078467**	**1.25**	**6.25**	**4.57**	**1.37**
NACHT, leucine rich repeat and PYD (pyrin domain) containing 1	**NALP1**	**NM_033007**	**1.00**	**5.74**	**2.41**	**2.38**
Zinc finger, DHHC domain containing 11	ZDHHC11	NM_024786	−1.06	5.56	4.78	1.16
Advillin	AVIL	NM_006576	1.13	5.16	3.73	1.38
Fas	FAS	NM_152873	−1.01	4.80	6.43	−1.34
Sestrin 2	SESN2	NM_031459	1.01	4.51	2.99	1.51
Tumor necrosis factor receptor superfamily, member 10a	**TNFRSF10A**	**NM_003844**	**1.74**	**4.50**	**2.15**	**2.09**
Heme oxygenase 1	**HMOX1**	**NM_002133**	**1.54**	**4.42**	**1.76**	**2.51**
Rho family GTPase 3	RND3	NM_005168	2.71	4.38	2.29	1.91
v-fos FBJ murine osteosarcoma viral oncogene homolog	FOS	NM_005252	−2.13	4.35	7.28	−1.67
Polo-like kinase 2	PLK2	NM_006622	1.97	4.35	3.44	1.26
Interleukin 8	IL8	NM_000584	1.06	4.31	9.32	−2.16
CDC-like kinase 1	CLK1	NM_004071	1.63	4.26	3.35	1.27
EPH receptor A2	EPHA2	NM_004431	1.19	4.17	2.86	1.46
Sphingomyelin synthase 2	SGMS2	NM_152621	1.20	4.09	5.65	−1.38
Erythrocyte membrane protein band 4.1 like 4A	EPB41L4A	NM_022140	1.10	3.63	1.70	2.14
Lymphocyte-specific protein 1	LSP1	NM_002339	1.81	3.63	3.21	1.13
Protein phosphatase 1D magnesium-dependent, delta isoform	PPM1D	NM_003620	1.04	3.63	4.74	−1.31
Connective tissue growth factor	CTGF	NM_001901	1.24	3.61	4.04	−1.12
UL16 binding protein 2	ULBP2	NM_025217	−1.09	3.60	4.66	−1.29
NFKB inhibitor interacting Ras-like 1	NKIRAS1	NM_020345	1.56	3.52	−1.19	4.19
Keratin associated protein 2–1	KRTAP2–1	NM_001123387	2.06	3.44	4.97	−1.44
Heparin-binding EGF-like growth factor	HBEGF	NM_001945	−1.46	3.32	2.79	1.19
Zinc finger protein ZNF468	ZNF468	NM_199132	2.05	3.29	3.13	1.05
Serine (or cysteine) proteinase inhibitor, clade B (ovalbumin), member 5	SERPINB5	NM_002639	1.20	3.23	2.92	1.11
Acidic repeat containing	ACRC	NM_052957	−1.93	3.13	4.70	−1.50
Activating transcription factor 4	ATF4	NM_001675	2.16	3.10	−2.76	8.56
Par-6 partitioning defective 6 homolog beta (C. elegans)	PARD6B	NM_032521	1.39	3.02	3.16	−1.05
Protein-O-mannosyltransferase 1	POMT1	NM_007171	−1.07	3.02	2.43	1.24
Interleukin 23, alpha subunit p19	IL23A	NM_016584	−1.51	3.01	3.75	−1.25

[a] 43 genes were up-regulated at least 3-fold in response to H_2O_2 treatment. Among these genes, 6 unidentified genes were not listed in the Table. Bold characters indicate genes further investigated by real-time PCR.
[b] Data are expressed as fold change, as compared to the control or AG + H_2O_2, respectively.

characterized by morphological changes, chromatin condensation (intact and fragmented) and PI staining. As shown in Figure 8, however, treatment of AGS cells with AG (50 μg/ml) significantly blocked H_2O_2-induced apoptosis, suggesting that AG blocks H_2O_2-induced cellular damage presumably acting as an anti-oxidant.

Discussion

Extracts from *G. uralensis* have been widely used in Korea for the treatment of gastric ulcer. However, the mechanisms by which these extracts exert their therapeutic effects are largely unknown. ROS can increase cell and tissue damage and disrupt the barrier function of epithelium

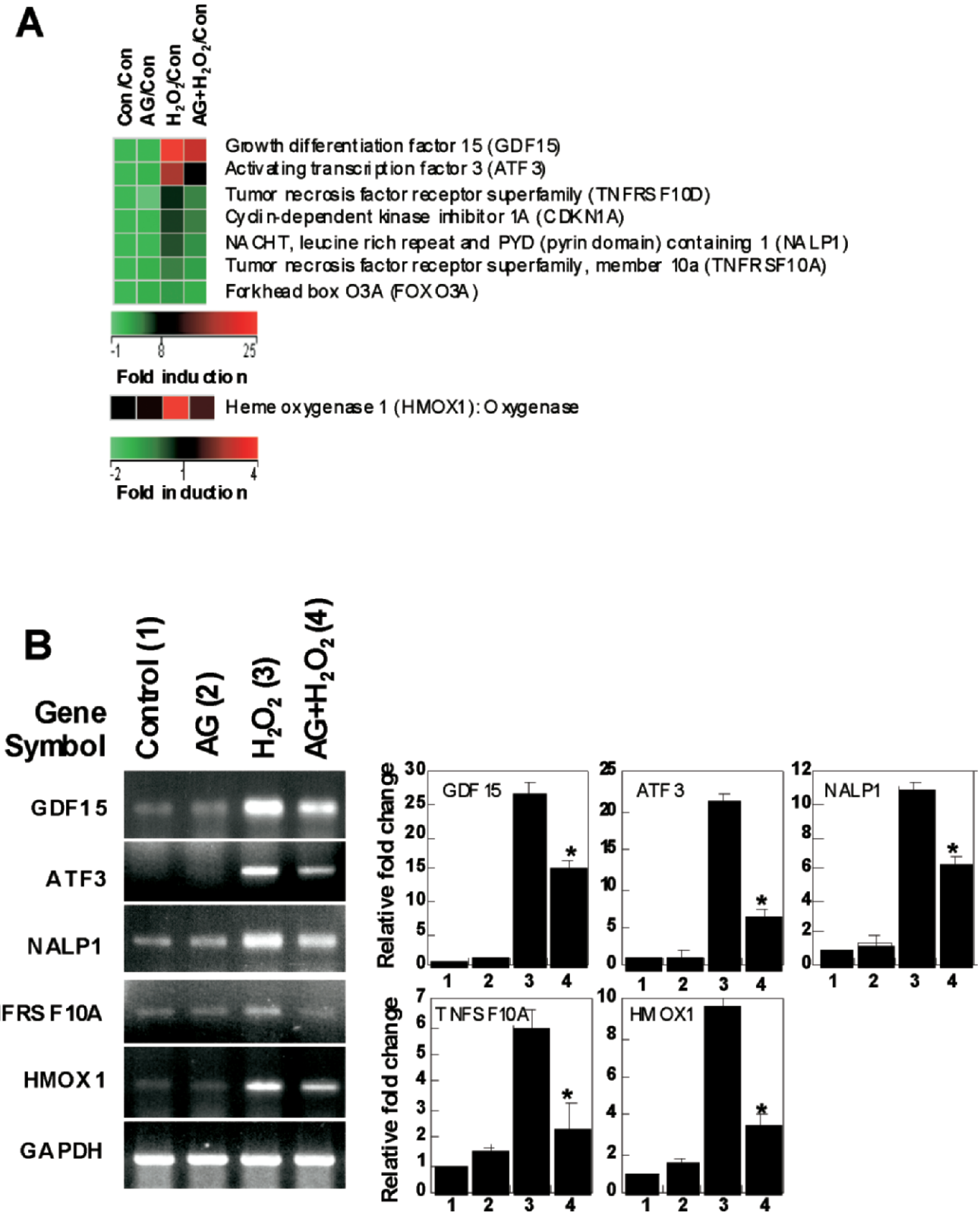

Figure 7. Cluster analysis of apoptotic cell death and oxidative stress-related genes and their validation by semi-quantitative RT-PCR and real-time RT-PCR. (A) Genes that are involved in apoptosis and oxidative stress. (B) The mRNA levels of selected genes (GDF15, ATF3, NALP1, TNFRSF10A, and HMOX1) were examined by RT-PCR (left) and real-time quantitative RT-PCR (right) as described in Materials and Methods. The real-time quantitative RT-PCR data shown represent the mean ± SD of three independent experiments. A color version of the figure is available in the online journal.

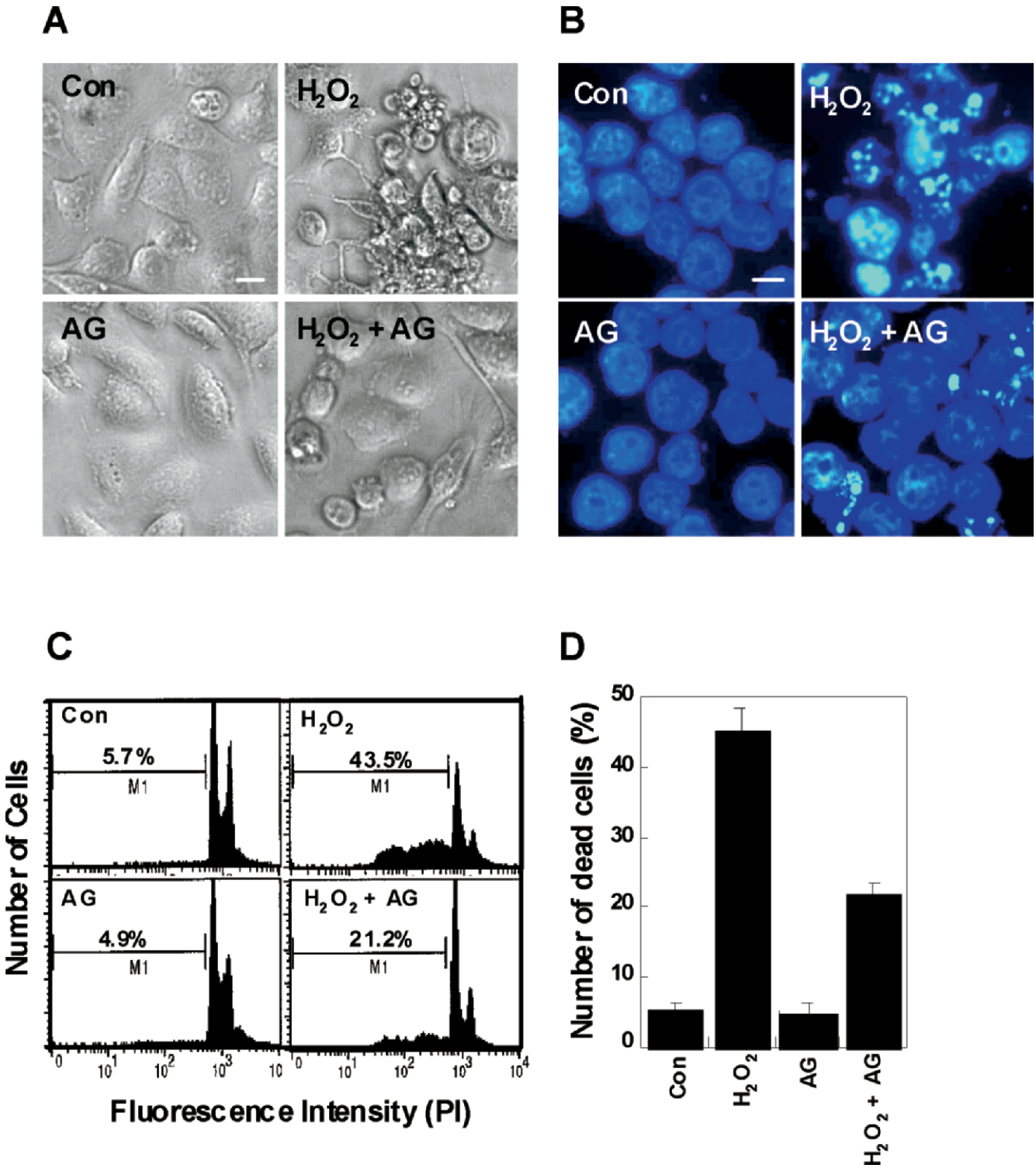

Figure 8. Effect of AG on H_2O_2-induced apoptotic cell death in AGS cells. AGS cells (1×10^5) were incubated for 1 h with AG (50 μg/ml), H_2O_2 (0.3 mM), or AG plus H_2O_2. Then, the cells were washed and incubated for 12 h with fresh complete medium containing 10% FBS. For AG-treated group, cells were washed and re-treated with AG (50 μg/ml) for 12 h except otherwise indicated. Characteristics of cell death were analyzed by morphological means, DAPI staining, and flow cytometric analysis. Cells were photographed with a phase-contrast microscope (×40) (A), or fixed in methanol, and stained with DAPI for the determination of nuclear condensation and fragmentation with a fluorescence microscope (×40) (B). Bars, 10 μm. (C) Cells were stained with PI as described in the Materials and Methods section. Then, the fluorescence intensities were analyzed by flow cytometer. Results are representative of three independent experiments (D). The bar graphs show the statistical results of (C). The data shown represent the mean ± SD of three independent experiments.

(4–6). It is well known that ROS increase the permeability of cultured epithelium by inducing disruption of actin cytoskeleton and morphological changes of cells, resulting in separation of adjacent cells (5). In the present study, we therefore screened four single compounds isolated from *G. uralensis* and one related compound by means of measuring their activity to protect H_2O_2-induced actin disruption in gastric epithelial AGS cells. We identified that AG potently blocked H_2O_2-induced actin disruption as well as cell death of AGS cells, suggesting a therapeutic effect of AG against gastric diseases related to the oxidative stress-induced mucosal damage.

A loss of gastric mucosal barrier integrity has been implicated as one of the key mechanisms underlying the pathophysiology of gastrointestinal (GI) diseases. Among them, gastroesophageal reflux disease (GERD) and peptic ulcer disease (PUD) are the most important and common GI disorders (32). Accordingly, characterizing a therapeutically effective means of protecting gastric barrier function under conditions of oxidant-induced injury, as the present investigation has done, is of significant clinical importance with potentially important implications for the treatment of a variety of oxidant-induced damages including GERD and PUD. Our data indicate that H_2O_2-mediated disruption of actin cytoskeleton in gastric epithelial cells is significantly blocked by AG treatment. In addition, treatment with AG inhibited $FeSO_4$-induced ROS generation in AGS cells, suggesting that AG acts as a strong anti-oxidant in AGS cells.

Genetic chip technology is characterized by high communication, low consumption and miniaturization (33, 34), providing a technological platform to study the mechanism of herbal medicines against various biological disorders including oxidative stress-related diseases. To gain molecular insight into the biological mechanisms played by AG in H_2O_2-induced cell damage, we investigated gene expression changes in response to AG in H_2O_2-treated gastric epithelial AGS cells using microarray technology. Among many of the gene expression changes observed, we found that genes involving in apoptosis or oxidative stress-dependent cell death pathways were most interesting as we focused our efforts on understanding the protective mechanism of AG against H_2O_2-induced cell damage. Five genes were chosen for confirmation through semi-quantitative RT-PCR and real-time PCR. Confirmation of the microarray trend of the five selected genes added confidence to the selections. It was interesting that all those genes involved in the apoptotic cell death were highly induced in response to the H_2O_2 treatment, but were significantly blocked by AG treatment. Among blocked genes by AG, GDF15, ATF3, and TNFRSF are known to be associated with p53-dependent apoptotic pathways in various cells (27–29). Since induction of p53 was accompanied by alterations of the mitochondrial potential and activation of the caspase-dependent apoptotic pathway, further experiments will be interesting to evaluate whether AG regulates the expression of these genes through modulation of p53-dependent pathways rather than working as a ROS scavenger. Among five genes confirmed, NALP1 contains a caspase-recruitment domain and has also been known to regulate caspase activation and apoptosis in injured neurons (35).

It was interesting to notice that HMOX1 is not induced by AG in AGS cells. Indeed, many reports have demonstrated that several antioxidants suppress cellular damages through the induction of HMOX1 (36, 37). Since HMOX-1 acts as a molecular anti-oxidant, it can also be imagined that AG protects AGS cells from H_2O_2 through the induction of HMOX-1 gene. However, our result that HMOX1 gene was suppressed by AG strongly suggests that the protective effect of AG in AGS cells is not related with the modulation of signaling pathways involved in HMOX1 gene induction but may directly scavenge ROS generated from hydrogen peroxide. In agreement with this result, our current results indicate that AG significantly blocks H_2O_2-induced apoptotic cell death in a dose relevant to the inhibition of H_2O_2-induced induction of HMOX-1 gene (Fig. 8).

Although not listed in this study, it was also interesting to note that some genes that encode cytoskeleton regulatory proteins were slightly down-regulated by H_2O_2 but recovered by AG. For example, KRTAP10–2 (keratin-associated protein), KRT6IRS (keratin 6 irs), ARP2/3 (actin related protein 2/3 complex), and KIFC2 (kinesin family member C2) were down-expressed ($<$2-fold) by H_2O_2 (data not shown). These results suggest that H_2O_2 treatment not only disrupts actin cytoskeleton but also reduces the level of cytoskeleton regulatory proteins, thus impairing the dynamics of epithelial cells. Expectedly, treatment with AG blocked the H_2O_2-induced down-expression of these genes, thereby further implying that AG could be a useful drug for the effective prevention of gastric mucosal damages by maintaining gastro-intestinal integrity against oxidative stresses.

Cell-based experiment is very valuable not only for rapid screening of potential therapeutic agents but also for gaining mechanistic insights not accessible otherwise. However, the observations made in cultured cells need to be confirmed using appropriate models. For example, one important issue raised in the current investigation is that all the cell culture was carried out at neutral pH, and yet the idea was to model peptic ulcer. As the stomach would have a far lower pH, it would be important to test whether the solubility of AG is similar at stomach pH and neutral pH. We therefore tested the solubility of AG in various pH conditions (pH 2.0–10.0) and observed that AG (ranged from 10 to 1000 μg/ml) was well solubilized even in low (pH 2.0) or high (pH 10.0) pH conditions, as determined by HPLC (data not shown) (38). In support of this result, AG is now commercially used as anti-inflammatory and anti-allergic remedy (13). This report implies that AG might be absorbed in the stomach pH well, as we already have seen in

neutral pH. Another important issue raised is that the current observations need to be confirmed using appropriate animal models to test *in vivo* significance. Indeed, *in vivo* efficacy testing of potential therapeutic agents is a prerequisite for their further development as clinically useful agents. Interestingly, it has been demonstrated that oral administration of AG in rat and mice experiments showed that the compound is related to practically nontoxic drugs (39). In addition, the authors used 7 mg/kg of AG as a therapeutic dose (39). As this concentration is approximately equal to the concentration of the 140 μg/mouse (~20 g), the present study implies an *in vivo* relevance of AG effect. In spite of this calculation, it would be important to examine whether the *in vitro* effects of AG have any relation to effects that might be seen following human consumption of an AG supplement.

Taken together, our current results describing the protective effect of AG against H_2O_2-induced cell damage and the global gene expression profiles in response to AG in H_2O_2-treated gastric epithelial AGS cells will contribute to the elucidation of the efficacy of AG in protecting gastric mucosal damages. Further, it implies that AG has a therapeutic activity for the treatment of diseases characterized by gastric mucosal ulceration. Additional studies will be required to evaluate whether AG has a potential to be developed for the therapeutic modality for the prevention of gastric mucosal ulceration as well as inflammation.

1. Fridovich I. Superoxide radical and superoxide dismutases. Annu Rev Biochem 64:97–112, 1995.
2. Manna SK, Aggarwal BB. Interleukin-4 down-regulates both forms of tumor necrosis factor receptor and receptor-mediated apoptosis, NF-kappaB, AP-1, and c-Jun N-terminal kinase. Comparison with interleukin-13. J Biol Chem 273:33333–33341, 1998.
3. Manna SK, Zhang HJ, Yan T, Oberley LW, Aggarwal BB. Overexpression of manganese superoxide dismutase suppresses tumor necrosis factor-induced apoptosis and activation of nuclear transcription factor-kappaB and activated protein-1. J Biol Chem 273:13245–13254, 1998.
4. Banan A, Fitzpatrick L, Zhang Y, Keshavarzian A. OPC-compounds prevent oxidant-induced carbonylation and depolymerization of the F-actin cytoskeleton and intestinal barrier hyperpermeability. Free Radic Biol Med 30:287–298, 2001.
5. Welsh MJ, Shasby DM, Husted RM. Oxidants increase paracellular permeability in a cultured epithelial cell line. J Clin Invest 76:1155–1168, 1985.
6. Banan A, Fields JZ, Zhang Y, Keshavarzian A. iNOS upregulation mediates oxidant-induced disruption of F-actin and barrier of intestinal monolayers. Am J Physiol Gastrointest Liver Physiol 280:G1234–1246, 2001.
7. Smoot DT, Elliott TB, Verspaget HW, Jones D, Allen CR, Vernon KG, Bremner T, Kidd LC, Kim KS, Groupman JD, Ashktorab H. Influence of Helicobacter pylori on reactive oxygen-induced gastric epithelial cell injury. Carcinogenesis 21:2091–2095, 2000.
8. Yoshida N, Yoshikawa T, Iinuma S, Arai M, Takenaka S, Sakamoto K, Miyajima T, Nakamura Y, Yagi N, Naito Y, Mukai F, Kondo M. Rebamipide protects against activation of neutrophils by Helicobacter pylori. Dig Dis Sci 41:1139–1144, 1996.
9. Suzuki M, Nakamura M, Mori M, Miura S, Tsuchiya M, Ishii H. Lansoprazole inhibits oxygen-derived free radical production from neutrophils activated by Helicobacter pylori. J Clin Gastroenterol 20 Suppl 2:S93–96, 1995.
10. Ilizarov AM, Koo HC, Kazzaz JA, Mantell LL, Li Y, Bhapat R, Pollack S, Horowitz S, Davis JM. Overexpression of manganese superoxide dismutase protects lung epithelial cells against oxidant injury. Am J Respir Cell Mol Biol 24:436–441, 2001.
11. Sakurai MH, Matsumoto T, Kiyohara H, Yamada H. Detection and tissue distribution of anti-ulcer pectic polysaccharides from Bupleurum falcatum by polyclonal antibody. Planta Med 62:341–346, 1996.
12. Hsiang CY, Lai IL, Chao DC, Ho TY. Differential regulation of activator protein 1 activity by glycyrrhizin. Life Sci 70:1643–1656, 2002.
13. Baltina LA. Chemical modification of glycyrrhizic acid as a route to new bioactive compounds for medicine. Curr Med Chem 10:155–171, 2003.
14. Yano S, Harada M, Watanabe K, Nakamaru K, Hatakeyama Y, Shibata S, Takahashi K, Mori T, Hirabayashi K, Takeda M, *et al.* Antiulcer activities of glycyrrhetinic acid derivatives in experimental gastric lesion models. Chem Pharm Bull (Tokyo) 37:2500–2504, 1989.
15. Arase Y, Ikeda K, Murashima N, Chayama K, Tsubota A, Koida I, Suzuki Y, Saitoh S, Kobayashi M, Kumada H. The long term efficacy of glycyrrhizin in chronic hepatitis C patients. Cancer 79:1494–1500, 1997.
16. van Rossum TG, Vulto AG, Hop WC, Schalm SW. Glycyrrhizin-induced reduction of ALT in European patients with chronic hepatitis C. Am J Gastroenterol 96:2432–2437, 2001.
17. Saitoh T, Shibata S. Chemical studies on the oriental plant drugs. XXII. Some new constituents of licorice root. (2). Glycyrol, 5-O-methylglycyrol and isoglycyrol. Chem Pharm Bull (Tokyo) 17:729–734, 1969.
18. Wang CL, Zhang RY, Han YS, Dong XG, Liu WB. [Chemical studies of coumarins from Glycyrrhiza uralensis Fisch]. Yao Xue Xue Bao 26: 147–151, 1991.
19. Yang L, Liu YL, Lin SQ. [HPLC analysis of flavonoids in the root of six Glycyrrhiza species]. Yao Xue Xue Bao 25:840–848, 1990.
20. Shim SB, Kim NJ, Kim DH. Beta-glucuronidase inhibitory activity and hepatoprotective effect of 18 beta-glycyrrhetinic acid from the rhizomes of Glycyrrhiza uralensis. Planta Med 66:40–43, 2000.
21. Kondratenko RM, Baltina LA, Mustafina SR, Vasil'eva EV, Pompei R, Deidda D, Pliasunova OA, Pokrovskii AG, Tolstikov GA. [The synthesis and antiviral activity of glycyrrhizic acid conjugates with alpha-D-glucosamine and some glycosylamines]. Bioorg Khim 30: 308–315, 2004.
22. Kondratenko RM, Baltina LA, Vasil'eva EV, Nasyrov Kh M, Kireeva RM, Baschenko N, Fridman SM, Tolstikov GA. [Synthesis and immunomodulating activity of new diglycopeptides of glycyrrhizinic acid and its 30-methyl ester]. Bioorg Khim 30:168–173, 2004.
23. Kondratenko RM, Baltina LA, Vasil'eva EV, Ismagilova AF, Nasyrov Kh M, Baschenko N, Kireeva RM, Fridman SM, Tolstikov GA. [Synthesis and immunostimulating activity of cysteine-containing glycopeptide derivatives of glycyrrhizic acid]. Bioorg Khim 30:61–67, 2004.
24. Royall JA, Ischiropoulos H. Evaluation of 2′,7′-dichlorofluorescin and dihydrorhodamine 123 as fluorescent probes for intracellular H2O2 in cultured endothelial cells. Arch Biochem Biophys 302:348–355, 1993.
25. Greene BT, Thorburn J, Willingham MC, Thorburn A, Planalp RP, Brechbiel MW, Jennings-Gee J, Wilkinson JT, Torti FM, Torti SV. Activation of caspase pathways during iron chelator-mediated apoptosis. J Biol Chem 277:25568–25575, 2002.
26. Banan A, Choudhary S, Zhang Y, Fields JZ, Keshavarzian A. Oxidant-induced intestinal barrier disruption and its prevention by growth factors in a human colonic cell line: role of the microtubule cytoskeleton. Free Radic Biol Med 28:727–738, 2000.
27. Kadara H, Schroeder CP, Lotan D, Pisano C, Lotan R. Induction of

GDF-15/NAG-1/MIC-1 in human lung carcinoma cells by retinoid-related molecules and assessment of its role in apoptosis. Cancer Biol Ther 5:518–522, 2006.

28. Mashima T, Udagawa S, Tsuruo T. Involvement of transcriptional repressor ATF3 in acceleration of caspase protease activation during DNA damaging agent-induced apoptosis. J Cell Physiol 188:352–358, 2001.
29. Ronchetti S, Zollo O, Bruscoli S, Agostini M, Bianchini R, Nocentini G, Ayroldi E, Riccardi C. GITR, a member of the TNF receptor superfamily, is costimulatory to mouse T lymphocyte subpopulations. Eur J Immunol 34:613–622, 2004.
30. Guyton KZ, Spitz DR, Holbrook NJ. Expression of stress response genes GADD153, c-jun, and heme oxygenase-1 in H2O2- and O2-resistant fibroblasts. Free Radic Biol Med 20:735–741, 1996.
31. Tyrrell R. Redox regulation and oxidant activation of heme oxygenase-1. Free Radic Res 31:335–340, 1999.
32. Pilotto A. Aging and upper gastrointestinal disorders. Best Pract Res Clin Gastroenterol 18 Suppl:73–81, 2004.
33. Schena M, Shalon D, Heller R, Chai A, Brown PO, Davis RW. Parallel human genome analysis: microarray-based expression monitoring of 1000 genes. Proc Natl Acad Sci U S A 93:10614–10619, 1996.
34. Lockhart DJ, Dong H, Byrne MC, Follettie MT, Gallo MV, Chee MS, Mittmann M, Wang C, Kobayashi M, Horton H, Brown EL. Expression monitoring by hybridization to high-density oligonucleotide arrays. Nat Biotechnol 14:1675–1680, 1996.
35. Frederick Lo C, Ning X, Gonzales C, Ozenberger BA. Induced expression of death domain genes NALP1 and NALP5 following neuronal injury. Biochem Biophys Res Commun 366:664–669, 2008.
36. Erdmann K, Grosser N, Schroder H. L-methionine reduces oxidant stress in endothelial cells: role of heme oxygenase-1, ferritin, and nitric oxide. AAPS J 7:E195–200, 2005.
37. Gao M, Kondo F, Murakami T, Xu JW, Ma N, Zhu X, Mori K, Ishida T. 1-Aminocyclopropanecarboxylic acid, an antagonist of N-methyl-D-aspartate receptors, causes hypotensive and antioxidant effects with upregulation of heme oxygenase-1 in stroke-prone spontaneously hypertensive rats. Hypertens Res 30:249–257, 2007.
38. Koga K, Kawashima S, Shibata N, Takada K, Murakami M. Preparation and rectal absorption of highly concentrated glycyrrhizin solution. Biol Pharm Bull 26:1299–1305, 2003.
39. Antov G, Khalkova Z, Mikhailova A, Zaikov K, Burkova T. [The toxicological characteristics of ammonium glycyrrhizinate (glycyram). A study of its acute and subacute toxicity]. Eksp Klin Farmakol 60:65–67, 1997.